Time-lapse OBN seismic data regularization using structural shaping model constraint: A modeling study on Brazilian Pre-salt.

Mesay G. Gebre* , Carlos A. N. da Costa, João M. de Araújo, Edwin F. Duarte, Danyelle da Silva

Universidade Federal do Rio Grande do Norte, Natal, RN, 59078-970, Brazil

This paper was prepared for presentation at the 18th International Congress of the Brazilian Geophysical Society, held in Rio de Janeiro, Brazil, 16-19 October, 2023.

Abstract

Seismic data regularization plays a fundamental role in time-lapse seismic cross-equalization processing workflow by disregarding spatial irregularity that is caused by the differences in spatial sampling. This improves the repeatability between different successive surveys. In this work, we discuss a regularization technique based on structural shaping model constraint with an iterative optimization strategy. We performed several numerical simulation tests by using synthetic time-lapse OBN data sets. All results show the capacity and practicality of the method in transforming spatially irregular data into regular data and which in turn shows the potential of the method in the reduction of non-repeatability in time-lapse data.

Introduction

Time-lapse (4D) seismic data is widely used for monitoring production-related changes in the reservoir. High repeatability is required between 4D surveys in order to obtain reasonable differences and allow for precise interpretation. However, several factors such as velocity variation in the near-surface, ambient noise, source and receiver location miss match, and other survey factors deteriorate the repeatability (Pevzner et al., 2011; Johnston, 2013). Particularly, irregular and sparse spatial sampling or missing traces caused by dead or severely bad traces, surface physical obstacles, and acquisition aperture between difference surveys are well-known problems in 4D interpretation and inversion by resulting artifacts (Pevzner et al., 2011; Zhou and Lumley, 2021). Therefore, data processing aimed at enhancing repeatability between surveys is extremely useful (Nguyen et al., 2015).

Generally, a cross-equalization process (Rickett and Lumley, 2001) is used to mitigate non-repeatability issues and hence improve the repeatability of 4D data. Seismic data regularization is one of the indispensable steps in cross-equalization processing workflows. It helps to mitigate the problem of spatial data irregularity or sparsity by transforming the irregular data into a uniform grid or filling in the missing traces (Johnston, 2013). Regularization and interpolation can be implemented to different data domains; for example, if there are missing receivers, data interpolation is applied on the shot gather, and vice versa. Many authors have reported the advantage of applying regularization, and recently, it has become an essential component of 4D seismic data processing (Rickett and Lumley, 2001; Johnston, 2013).

Several kinds of seismic data regularization methods, based on different theories, have been developed by different scholars. Commonly used seismic data regularization techniques are mainly based on the different transforms for example Fourier transform (Jin, 2010), Radon transform (Gong et al., 2016), Seislet transform (Gan et al., 2015), Curvelet transform (Zhang et al., 2019). To have a general overview of the different methods we refer the readers to Wang and Yu (2021) and Cao et al. (2018).

In the present work, we discuss and apply seismic data regularization technique, to improve the repeatability of 4D ocean-bottom node (OBN) data, where the irregularly sampled data is transformed to the regularly spaced data by filling missing traces. The method is based on structural shaping model constraint with an iterative optimization strategy. We use a velocity model of the Brazilian Pre-salt in Santos Basin to generate the synthetic data sets.

Methodology

Seismic data regularization is an inverse problem and can be formulated by the following linear system of equations

$$\mathbf{d^{obs}} = \mathbf{Ld} \tag{1}$$

where $\mathbf{d}^{obs}$ is the observed data measured at irregular or sparse locations, $\mathbf{L}$ is a sampling operator and $\mathbf{d}$ represents the desired complete data. The sampling operator $\mathbf{L}$ is a diagonal matrix consists of 1 (representing observed grid points) and 0 (representing the missing trace). It is well known that solving Equation 1 for $\mathbf{d}$ is an ill-posed problem, thus the general strategy to find the solution is to formulate it into an optimization problem, by adding a stabilization term (Chen et al., 2019; Huang, 2022)

$$\widehat{\mathbf{d}} = \|\mathbf{d}^{obs} - \mathbf{Ld}\|_2^2 + \lambda \mathbf{S}(\mathbf{d}) \tag{2}$$

In Equation 2, the first term is the l_2 norm misfit function, which measures the proximity of the recovered data with observed data, $\mathbf{S}(\mathbf{d})$ is stabilization term or model constraint that is required to guarantee the stability of the solution by adding prior information to the solution and, λ is the trade-off parameter balancing the misfit and the stabilization. Several kinds of stabilization methods or model constraints $\mathbf{S}(\mathbf{d})$ have been proposed and used for seismic data regularization or interpolation. For example, Minimum weighted norm (Liu and Sacchi, 2004), sparsity-promoting constraints based on different transforms (Wang and Yu, 2021; Zhang and Lu, 2014), low-rank-based constraints (Wu and Bai, 2018). In recent years, the shaping model constraint (Fomel, 2007), a similar strategy to the one used in this work, has also been introduced into seismic data regularization and interpolation. The Shaping stabilization approach provides us a way to solve Equation 2 in an iterative framework, where stabilization or the addition of prior information is achieved by a shaping operator. Consider a shaping operator $\mathbf{S}$, the iterative solution for the optimization problem in Equation 2 can be expressed as (Fomel, 2007; Huang, 2022):

$$\mathbf{d}_{i+1} = \mathbf{S}\mathbf{d}_i - \lambda \mathbf{A}(\mathbf{d}^{obs} - \mathbf{L}\mathbf{d}_i)] \tag{3}$$

where $\mathbf{A}$, is a backward operator which provides a mapping from the fitting error space (i.e., the difference between the observed data $\mathbf{d}^{obs}$ and forward data $\mathbf{L}\mathbf{d}_i$ to the model space $\mathbf{d}_i$ (Chen et al., 2014). In the current work, we specifically use $\mathbf{A} = \mathbf{L}^T$ and the structural shaping operator introduced by (Chen et al., 2019):

$$\mathbf{S} = \mathbf{M}\mathbf{G}\mathbf{G}^{\mathbf{T}}\mathbf{M}^{\mathbf{T}} \tag{4}$$

where $\mathbf{M}$ is a summation operator, which corresponds to averaging the traces along the structural direction. $\mathbf{M}^T$ is its adjoint operator, which extends a trace to a group of traces along the structural direction so that the triangle smoothing operator can be applied along the structural direction and is called an extension operator $\mathbf{G}$ is a triangle smoothing operator (Xue et al., 2016), and G^T denotes its transpose or its adjoint operator. A more detailed discussion of the iterative optimization process with shaping stabilization framework to solve Equation 2 is given in Chen et al. (2019) and Huang (2022).

Numerical examples

In this section, we present a numerical simulation test example by applying the regularization method described above to improve the repeatability of 4D OBN synthetic data. To measure the regularization performance quantitatively, and also the quality of the reconstructed data after regularization, we use the Signal-to-Noise Ratio SNR which is expressed as (Wang and Yu, 2021): $SNR = \frac{\|\mathbf{d}^{exa}\|_2}{\|\mathbf{d}^{exa} - \mathbf{d}\|_2}$, where $\mathbf{d}^{exa}$ is the exact complete regular data and $\mathbf{d}$ represents the output of the regularization. In addition, we use the typical metric Normalized Root Means Square difference $NRMS$ also known as repeatability (Kragh and Christie, 2002) between the base and monitor data.

We used a realistic P-wave velocity model of the Brazilian Pre-salt in Santos Basin to generate the baseline and monitor data sets. Displayed in Figures 1a and 1b are the baseline and the perturbation P-wave velocity models respectively. The monitor velocity model is obtained by adding the perturbation (Figure 1b) to the baseline to mimic production-related change.

The synthetic data sets are computed by acoustic finite-difference modeling with 6.5 Hz peak frequency Ricker wavelet and 5 millisecond sampling. The acquisition geometry consisted of 51 nodes and 501 shots. The baseline survey was modeled with a regular node spacing

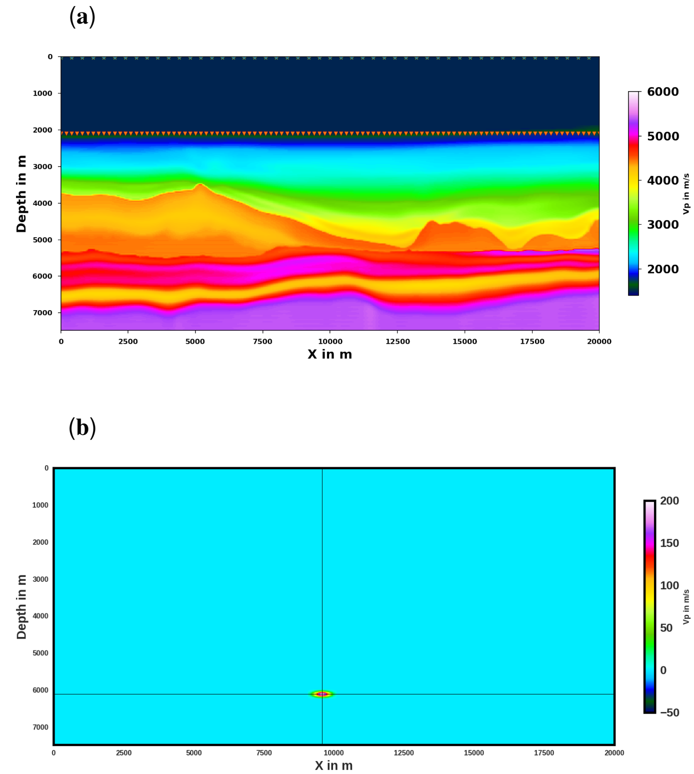

Figure 1: (a) The baseline P-wave velocity model. (b) P-wave velocity change added baseline to generate a monitor model.

of 400 m placed at the ocean bottom and source spacing of 40 m. The monitor data is modeled after adding the perturbation (Figure 1b) to the baseline velocity model and using the same source and receiver position. Figures 2a and 2b show an example of a central-node gather from the monitor data and the corresponding $f-k$ spectrum of the data. All the data presented here are normalized by their maximum absolute value. One can clearly observe different complex events from Figure 2a, which are caused by the complex geological structures of the Brazilian Pre-salt (Krueger et al., 2018). The computed $NRMS$ between the base and the full (exact) monitor is 0.153 %.

In order to consider non-repeatability, the monitor data subset was decimated by randomly removing 20 % of the traces in the receiver gather, to model non-repeatability caused by missing traces or irregular spatial sampling of the data due to bad trace removal and acquisition obstacles in real scenarios. The decimated data and the associated $f-k$ spectrum are shown in Figures 3a and 3b respectively. One can clearly observe the aliasing of non-repeatable monitor data from the $f-k$ amplitude spectrum in Figure 3b. As expected for the irregularly decimated data $NRMS$ value is large having a value of 21.725 % indicating the Non-repeatability effect. Moreover, the calculated SNR of the decimated monitor data is 3.05 dB.

The result of the regularization of the decimated monitor and its $f-k$ spectrum, by utilizing the method described in the methodology section, are shown in Figures 4a and 4b. As we can see from the $f-k$ amplitude spectrum of the regularized data (Figure 4b) spatial aliasing is removed and it is the same as the original data (Figure 2b). As

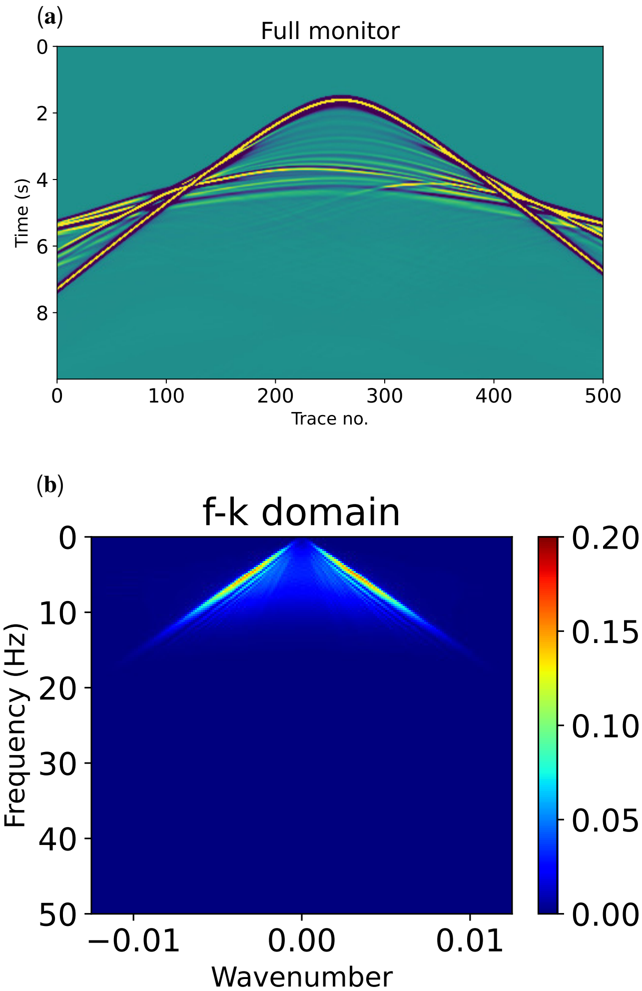

Figure 2: (a) Full monitor data from the central node. (b) $f-k$ amplitude spectrum of the full data.

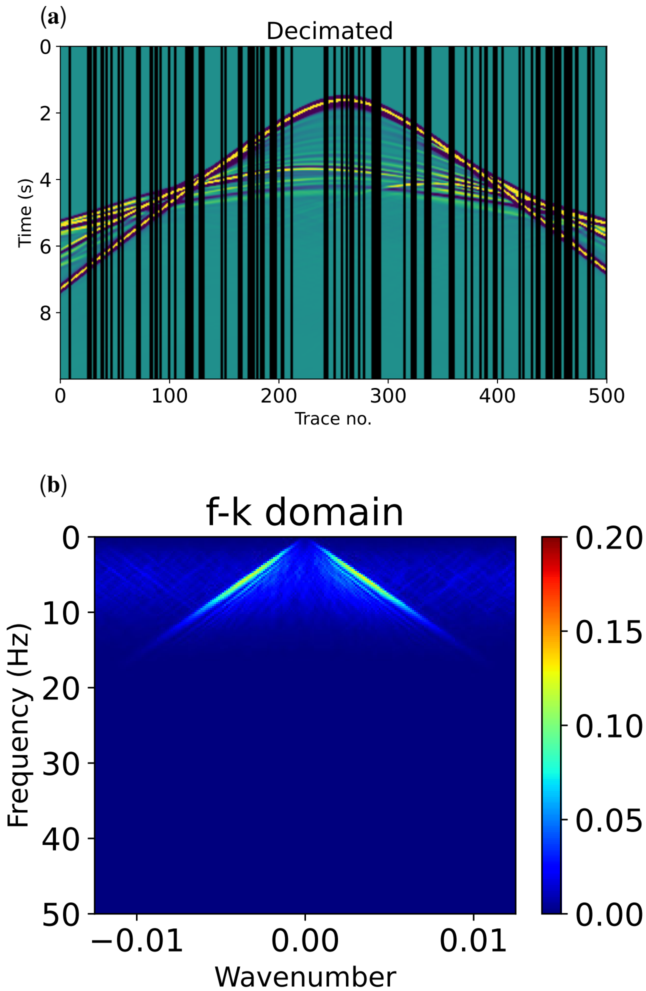

Figure 3: (a) Non-repeatable decimated data (obtained by randomly removing 20% traces) with $SNR = 3.05dB$. (b) $f-k$ amplitude spectrum of the decimated data)

compared to the SNR value of the decimated data, the computed SNR of the regularized data is very high having a $14.65\ dB$. It clearly indicates the improvement in SNR after the regularization process. The residual of the original full and regularized result is depicted in Figure 5a, which also reflects the precision of the reconstructed result with the negligible reconstruction error. Finally, we computed $NRMS$ between the baseline and the regularized data. As we aimed the $NRMS$ is highly improved having a value of approximately 0.386% and hence the method's performance in giving a reasonable result. In order to illustrate the effectiveness of the method more, we displayed a single-trace amplitude comparison in Figure 5b. The two traces are extracted from the middle trace (the 250th trace) of the complete original data and the regularized data. In this Figure, the blue and red lines are very close to each other.

Conclusion

In this work, we discussed seismic data regularization method, which is a component of cross-equalization workflow, to improve the repeatability of Time-laps data. The approach incorporates structural shaping model constraints to solve the stabilized inversion problem by using an iterative optimization strategy. The numerical simulation results presented here and other tests that are not presented show the method's performance in giving a reasonable result. Thus the methodology can be used as one component of the cross-equalization workflow to improve the repeatability in time-lapse OBN data by reconstructing and filing the irregularly missing seismic traces. Here, we showed only the application of the method on synthetic data, real application results will be shown in future works.

ACKNOWLEDGMENTS

The authors would like to acknowledge and give their warmest thanks to the support from Shell Brazil through the New computationally scalable methodologies for target-oriented 4D seismic in pre-salt reservoirs project at the Federal University of Rio Grande do Norte and the strategic importance of the support given by the Brazilian National Agency for Petroleum, Natural Gas, and Biofuels (ANP) through the R&D levy regulation.

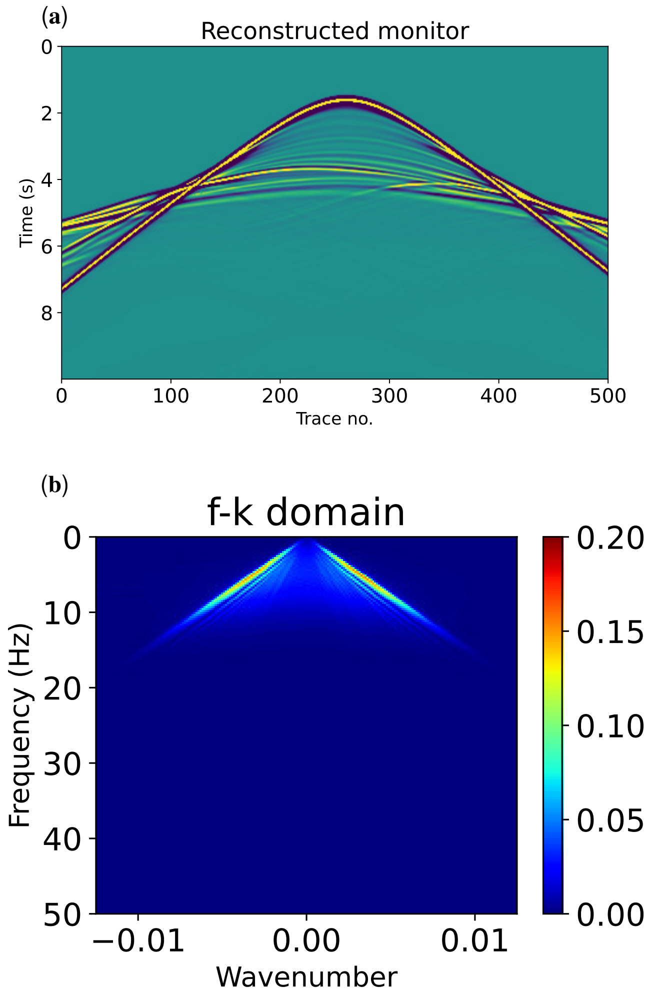

Figure 4: (a) The regularized result. (b) $f-k$ amplitude spectrum of the regularized data.

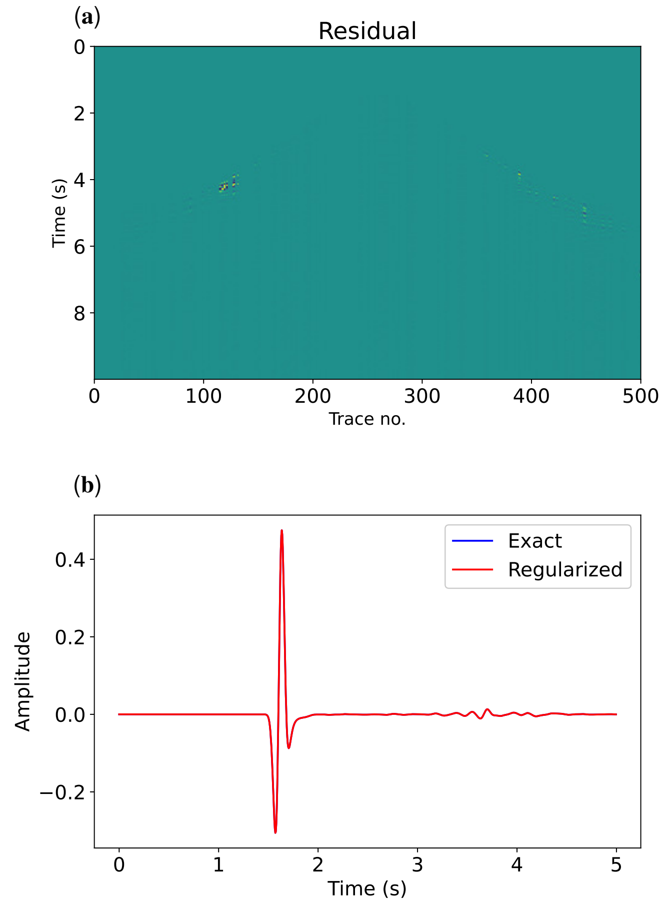

Figure 5: (a) Residual of the original full monitor data and regularized data. (b) Single-trace comparison of the original full and regularized data for the middle trace.

References

Cao, A., Stump, B., and DeShon, H., 2018, High-resolution seismic data regularization and wavefield separation: Geophysical Journal International, **213**, no. 1, 684–694.

Chen, Y., Fomel, S., and Hu, J., 2014, Iterative deblending of simultaneous-source seismic data using seislet-domain shaping regularization: Geophysics, **79**, no. 5, V179–V189.

Chen, Y., Chen, X., Wang, Y., and Zu, S., 2019, The interpolation of sparse geophysical data: Surveys in Geophysics, **40**, 73–105.

Fomel, S., 2007, Shaping regularization in geophysical-estimation problems: Geophysics, **72**, no. 2, R29–R36.

Gan, S., Wang, S., Chen, Y., Zhang, Y., and Jin, Z., 2015, Dealiased seismic data interpolation using seislet transform with low-frequency constraint: IEEE Geoscience and remote sensing letters, **12**, no. 10, 2150–2154.

Gong, X., Yu, S., and Wang, S., 2016, Prestack seismic data regularization using a time-variant anisotropic radon transform: Journal of Geophysics and Engineering, **13**, no. 4, 462–469.

Huang, W., 2022, Seismic data interpolation by shannon entropy-based shaping: IEEE Transactions on Geoscience and Remote Sensing, **60**, 1–12.

Jin, S., 2010, 5d seismic data regularization by a damped least-norm fourier inversion: Geophysics, **75**, no. 6, WB103–WB111.

Johnston, D. H., 2013, Practical applications of time-lapse seismic data: Society of Exploration Geophysicists.

Kragh, E., and Christie, P., 2002, Seismic repeatability, normalized rms, and predictability: The leading edge, **21**, no. 7, 640–647.

Krueger, J., Donno, D., Pereira, R., Mondini, D., Souza, A., Espinoza, J., and Khalil, A., 2018, Internal multiple attenuation for four presalt fields in the santos basin, brazil: Internal multiple attenuation for four presalt fields in the santos basin, brazil:, 2018 SEG International Exposition and Annual Meeting.

Liu, B., and Sacchi, M. D., 2004, Minimum weighted norm interpolation of seismic records: Geophysics, **69**, no. 6, 1560–1568.

Nguyen, P. K., Nam, M. J., and Park, C., 2015, A review on time-lapse seismic data processing and interpretation: Geosciences Journal, **19**, 375–392.

Pevzner, R., Shulakova, V., Kepic, A., and Urosevic, M., 2011, Repeatability analysis of land time-lapse seismic data: Co2crc otway pilot project case study: Geophysical prospecting, **59**, no. 1, 66–77.

Rickett, J., and Lumley, D., 2001, Cross-equalization data processing for time-lapse seismic reservoir monitoring: A case study from the gulf of mexico: Geophysics, **66**, no. 4, 1015–1025.

Wang, X., and Yu, S., 2021, Seismic data regularization on nonequispaced grid via a joint sparsity-promotion method: IEEE Geoscience and Remote Sensing Letters, **19**, 1–5.

Wu, J., and Bai, M., 2018, Adaptive rank-reduction method for seismic data reconstruction: Journal of Geophysics and Engineering, **15**, no. 4, 1688.

Xue, Z., Chen, Y., Fomel, S., and Sun, J., 2016, Seismic imaging of incomplete data and simultaneous-source data using least-squares reverse time migration with shaping regularization: Geophysics, **81**, no. 1, S11–S20.

Zhang, Y.-Q., and Lu, W.-K., 2014, 2d and 3d prestack seismic data regularization using an accelerated sparse time-invariant radon transform: Geophysics, **79**, no. 5, V165–V177.

Zhang, H., Diao, S., Chen, W., Huang, G., Li, H., and Bai, M., 2019, Curvelet reconstruction of non-uniformly sampled seismic data using the linearized bregman method: Geophysical Prospecting, **67**, no. 5, 1201–1218.

Zhou, W., and Lumley, D., 2021, Nonrepeatability effects on time-lapse 4d seismic full-waveform inversion for ocean-bottom node datanr effects on 4d fwi: Geophysics, **86**, no. 4, R547–R561.